CASE REPORT

3D segmentation and 3D printing in presurgical planning and patient education in sinonasal tumoral pathologies

Mihai Dragomir[1,2], **Codrut Sarafoleanu**[2,3], **Eduard Liciu**[1], **Daniel Cristea**[1]

[1]Center for Innovation and e-Health, "Carol Davila" University of Medicine and Pharmacy, Bucharest, Romania

[2]ENT&HNS Department, "Sfanta Maria" Hospital, Bucharest, Romania

[3]"Carol Davila" University of Medicine and Pharmacy, Bucharest, Romania

ABSTRACT

Digital planning and 3D printing have seen a significant impact in personalised presurgical planning in ENT pathology. However, segmentation and 3D printing of the cranium and especially the sinuses in ENT sinonasal pathologies are still fraught with challenges. This article will provide a comprehensive analysis, from segmentation to 3D printing, to provide insights into the future directions of 3D printing in sinonasal pathology and its implications for patient care.

KEYWORDS: 3D printing, sinonasal pathology, surgery.

INTRODUCTION

In recent years, the medical field has witnessed remarkable advancements with the integration of 3D printing (3DP) technology, with ample uses seen in both research and integrated medical applications. Multiple medical fields have inserted 3DP protocols in their workflow, particularly in personalized presurgical planning, and surgical guide and implant manufacturing. These advancements have revolutionized diagnostic and therapeutic approaches, enabling more precise and tailored treatment.

In ENT surgery, the utilization of 3DP for the segmentation and analysis of sinonasal structures offers unprecedented accuracy in understanding complex anatomical variations and disease manifestations, especially when approaching complex tumoral pathologies. The use cases are extremely complex and varied. 3D printed presurgical models can be fabricated with the intended use as aid for the surgical team. These models enable precise visualization of complex sinonasal structures, allowing surgeons to meticulously plan and simulate surgical procedures, thus enhancing accuracy and reducing intraoperative risks. 3DP technologies, such as Multi-Material FDM (Fused Deposition Modelling) and Material Jetting, can provide multi-coloured 3D models, emphasising, for example, different vascular and nervous structures that surround a sinonasal tumour[1]. Another use case is for patient education, where having tangible models serves as an invaluable tool for explaining intricate anatomical and pathological details, thereby improving patient comprehension and compliance to their treatment plan[2,3]. The use of 3DP models also extends to medical training, where they facilitate hands-on practice for medical students and residents, offering a realistic and safe environment to hone their skills before operating on actual patients. The ability of 3DP to create intricate structures inside the volume of a model opens the possibility of recreating the complex bone structures found in the skull base, such as mastoid cell structures[4], nasal cavity and paranasal sinuses[5].

The concept of "personalized medicine" has become increasingly prevalent in contemporary medical practice, aiding in the paradigm shift towards personalised, bespoke surgical treatments. Leveraging the inherent adaptability of 3DP technologies, personalized surgical guides can be produced to match the distinct anatomical structures of each patient. These customized guides aid surgeons in navigating complex and intricate ana-

Corresponding author: Mihai Dragomir, ENT Resident, ENT&HNS Department, CESITO Center, "Sfanta Maria" Hospital, Bucharest, Romania
Address: 37-39 Ion Mihalache Blvd, District 1, Bucharest, Romania
ORCID: https://orcid.org/0009-0007-3841-6748
e-mail: mihai.dragomir@umfcd.ro
Received for publication: April 2, 2024 / **Accepted:** May 10, 2024

tomical regions during sinonasal surgeries, thereby enhancing surgical precision, reducing the duration of operative procedures.

Finally, 3DP surgical implants are setting new standards in post-traumatic and oncological maxillofacial reconstruction, with metallic bespoke designs created to perfectly replace osseous structures, post-resection, to ensure optimal fit and function, significantly improving postoperative outcomes. The customization capabilities of 3D printing allow the production of perfectly shaped biocompatible implants that integrate seamlessly with the patient's native tissues, reducing the risk of complications and promoting faster recovery[6-10].

However, despite its transformative potential, the application of 3D printing in this specialized area is not without challenges, particularly in oncological cases of the sinonasal region.

Sinonasal tumours encompass a wide range of presentations and variations, which require meticulous evaluation and management. 3D segmentation is the process in medical imaging that transforms raw data from CT (Computed Tomography) and MRI (Magnetic Resonance Imaging) scans into detailed, three-dimensional representations of anatomical structures. The process begins with the acquisition of high-resolution imaging data, which captures fine details of the internal anatomy. Using specialized software, the images undergo a process of filtering and 3D stacking, called segmentation, a step that involves delineating the boundaries of various tissues and structures within the scans. If more images are provided (that is to say, the images have a small spacing – distance between consecutive images – and slice thickness – thickness of the body that is encompassed into each 2D image), then the final model is much more detailed. This segmentation is often facilitated by algorithms that can automatically detect and differentiate between different types of tissues based on their unique radiodensity or signal intensity profiles – these differences show up on the 2D images of the scans as different intensities of White, Gray and Black. Once the segmentation is complete, the software reconstructs these segmented regions into a 3D model, allowing for comprehensive visualization of the entire structure. This 3D model can be further refined and annotated to highlight specific areas of interest, such as tumours, vascular structures, a process that is impossible to do on normal 2D CT images.

Once these initial 3D digital models are built, they undergo post-processing, separation of areas of interest, and surgical guide or implant design. The presence of metal inside the body can often create artifacts in the CT image, which need to be sorted out before the final model can be 3D printed. The final resulting 3D model is a 1:1 representation of the specific anatomy of each patient. Depending on the intended use case of the model, various 3D printing technologies can be then employed for the physical production.

Because of the inherent geometrical complexity of the sinonasal region, several challenges arise in the practical implementation of 3D printing for sinonasal pathologies. These include the need for high-resolution imaging to capture fine anatomical details, particularly around the anatomical structures of the skull base. Differentiating pathological tissues from surrounding structures presents supplemental challenges, especially when trying to separate fine bone structures, such as those seen in sinus walls from intrasinusal tumours. These structures, because of their small size and thinness, often are not capable of absorbing enough radiation during CT scan, resulting in a lower, gray tone on the image, very much like that of the surrounding soft tissue. While the advent of modern artificial intelligence (AI) driven segmentation tools has reduced the level of errors, and new methods of segmentation, including the use of air as a masking tool have improved resulting 3D models, manual validation is still a must.

We present a series of cases of sinonasal tumours and post-excision reconstructions that underwent presurgical planning, the challenges faced with segmenting and 3D printing these complex structures, and various mitigation methods.

CASE REPORT

Case 1

The first patient, a 34-year-old male, presented with nasal obstruction, pain in the left ethmoidal and frontal sinus points, and recurrent anterior epistaxis. The primary investigation revealed the presence of a sinonasal tumour in the left nasal cavity, located in the upper two-thirds of the left nasal airway. To assess the tumoral extension, high-resolution cranio-facial computed tomography (CT) scans were used to obtain detailed images of the sinonasal region. The CT evaluation revealed the presence of the tumour in the upper two-thirds of the left nasal fossa with extension in the adjacent anterior left ethmoidal cells, with some small tumour buds extending towards the left maxillary sinus and the left half of the frontal sinus (Figure 1). Also, the tumour invaded the left nasolacrimal duct, the lacrimal sac, the lamina papyracea posterior to it, but without infiltration of the extrinsic eye muscles. Erosion of the nasal septum, extending 2-3 mm towards the right nasal fossa, the cribriform plate, predominantly on the left side, and invasion of the left olfactory fossa were also observed. CT imaging did not reveal any invasion of the adjacent frontobasal brain parenchyma. Images were taken at a slice thickness of 1.25 mm and slice spacing of 0.625 mm.

The segmentation of the tumour presented significant challenges due to its close proximity to surrounding soft structures. These structures, characterized by their soft tissue density and complex anatomical variations, posed dif-

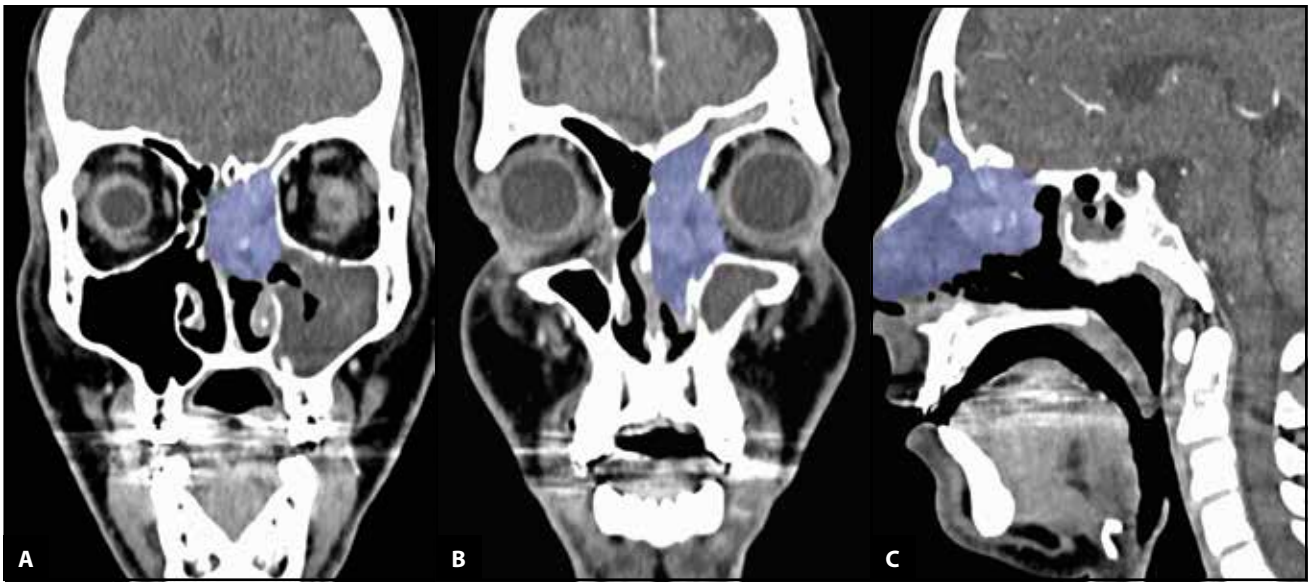

Figure 1. Cranio-facial CT images showing the tumour (purple highlight) in coronal (images **A, B**) and sagital (image **C**) incidences.

ficulties in distinguishing tumour boundaries accurately. Additionally, the tumour's proximity to the orbit necessitated careful consideration to avoid inadvertent inclusion of these vital structures in the segmentation process.

3D Slicer, an open-source segmentation software was used[11]. Initial segmentation was performed using simple threshold limits, which netted the primary 3D model of the skull. The model's output was then refined manually to ensure precise delineation of the tumour boundaries. Particular attention was paid to the ethmoidal and orbital walls, which required meticulous separation due to their intricate and overlapping nature.

The resulting 3D model was post-processed using Blender, an open-source 3D editing software[12], to remove

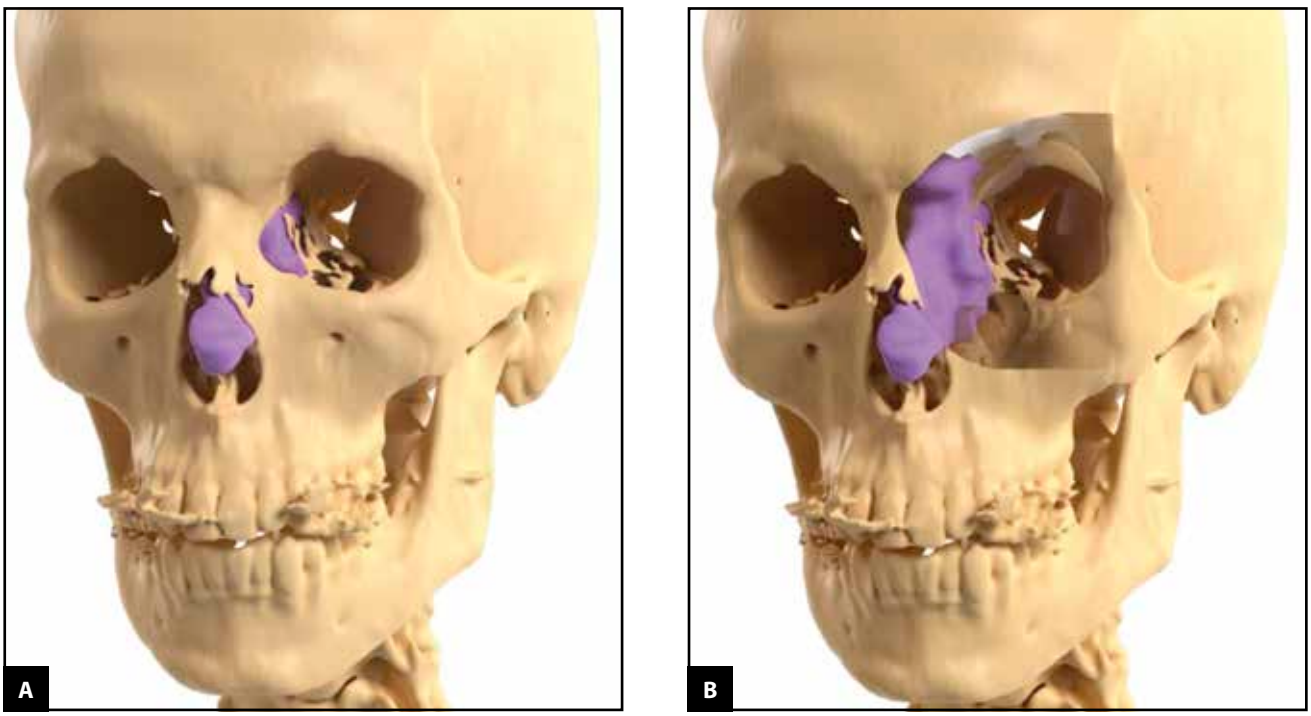

Figure 2. 3D models of the left sinonasal tumour (purple) (histopathologic results: neuroblastoma) showing erosion of the left orbital medial wall **(A)** and extension into the frontal sinus (via cutout) **(B)**.

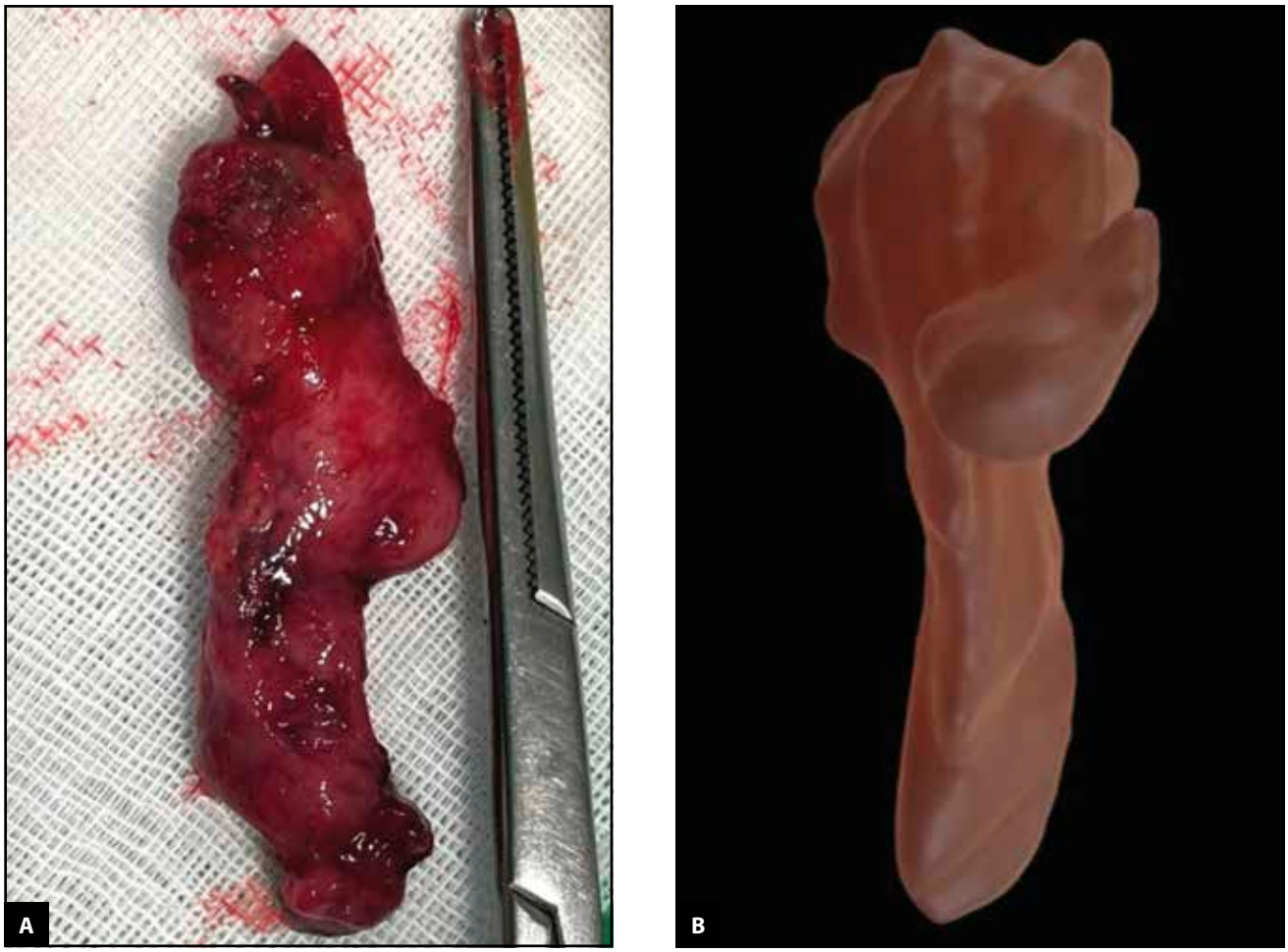

Figure 3. Visual comparison between the excised tumor **(A)** and the 3D digital model **(B)**.

artefacts and prepare the model for 3D printing. The purpose of the model was presurgical assessment of the extent of the tumour. For this purpose, the 3D digital model allowed a separation and virtual removal of part of the bone structures surrounding the tumour, to better extension and invasion. Final image renders were also performed in Blender (Figure 2).

For the physical production of the model, two technologies were chosen from those available in our laboratory. Fused Deposition Modelling Multi Material 3D printing was elected for one model, as it offered the possibility of 3D printing the model in multiple colours, to better emphasise and separate the anatomical structures from the tumour. The models were 3D printed on Bambu Lab P1P 3D printer, with AMS multi-material module, Bambu Studio as slicing software, at a layer height of 0.18 mm[13], using PLA (Polylactic Acid) filaments. 3D printing of the model presented challenges, mainly due to the intricate structures of the skull base. A second model was printed on MSLA (Masked Stereolithography) 3D printing technology. The 3D printer chosen was a Anycubic Mono X2, using Anycubic Gray V2 resin[14]. This 3D printing technology uses a UV light source that passes through an LCD screen (a mask) and into a vat of photopolymer resin. This resin hardens when exposed to UV light. This technology was chosen because it was able to provide a very detailed model, with a minimal pixel size of 50µm. A layer height of 50µm was chosen.

The surgical outcome using presurgical planning was positive, with the entire tumour being removed via transnasal endoscopic approach. After the excision of the nasosinusal tumour, visual comparison was conducted between the physical specimen and the 3D digital model obtained through segmentation. The excised tumour was found to closely resemble the digital reconstruction in both size and shape (Figure 3). The 3D model, generated from preoperative imaging data, provided a highly accurate representation of the tumour's dimensions and morphology.

Case 2

The second case involved a 38-year-old female patient with bilateral ethmoidal osteoma, presenting in our clinic for evaluation after initial investigation, 1 year prior. Because of the inherent slow progression of the benign tumour, yet with severe consequences if left unattended, we

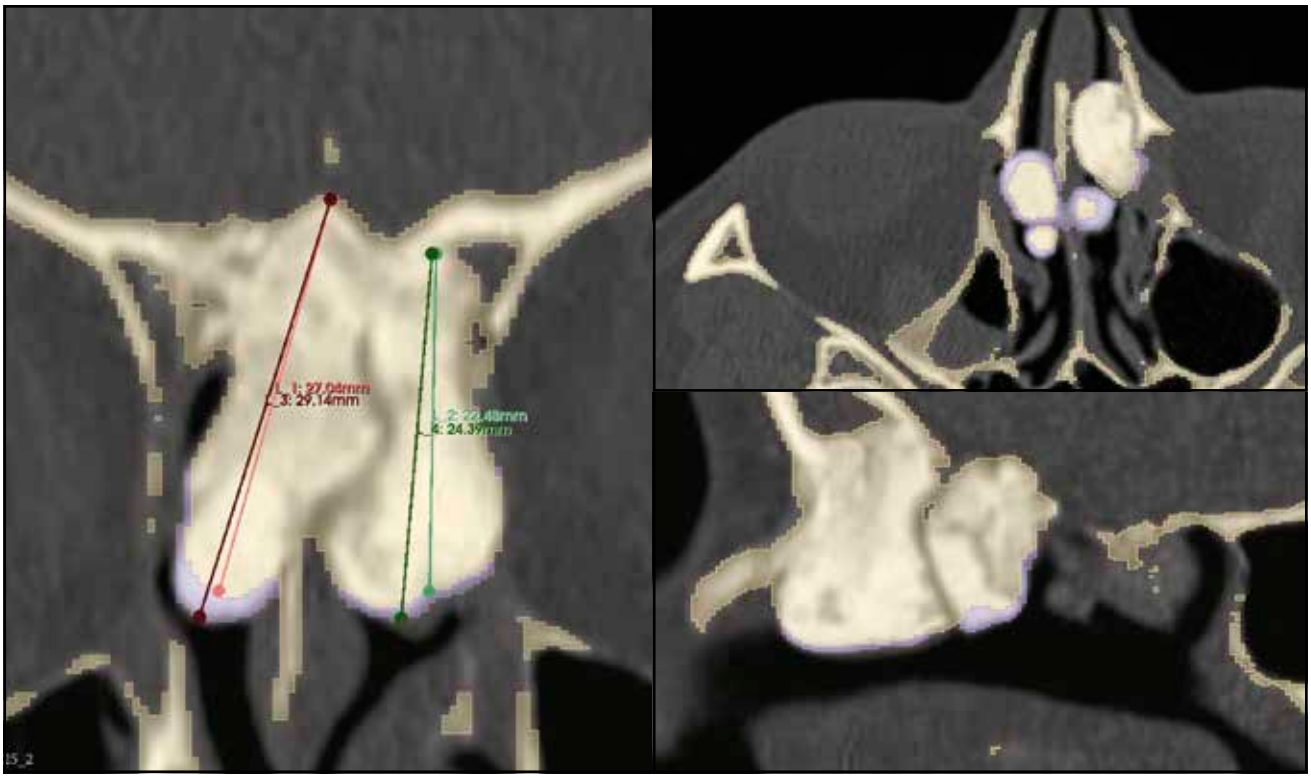

Figure 4. High-resolution cranio-facial CT scans (coronal, axial, sagittal): Highlights of the osteoma showing initial dimensions at presentation (yellow shading) and evolution after 1 year (purple shading).

proposed a 3D reconstruction of both cranio-facial CT scans, taken precisely 1 year apart, in order to better evaluate the extension of the disease (Figure 4).

High-resolution cranio-facial CT scans were performed on an GE Optima CT660 CT Scanner at a slice thickness of 0.625 mm and a slice spacing of 0.312 mm. The resulting CT scans were then imported into 3D Slicer. For the first step, alignment of the two CT scans was performed. The two acquisitions were both performed at identical parameters of slice thickness, spacing and kernel filtering. Because of that, the only requirement was a positional transformation of one of the CT

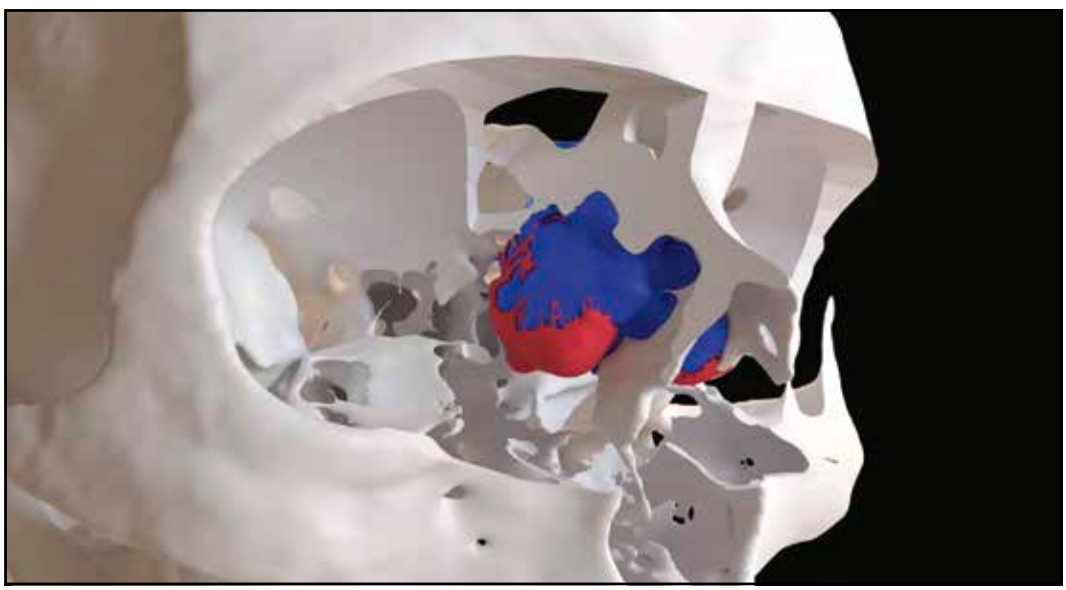

Figure 5. 3D render of the osteoma, with part of the orbit removed (white) to allow for better visualisation of the tumor (blue) and the extension over a period of 1 year (red).

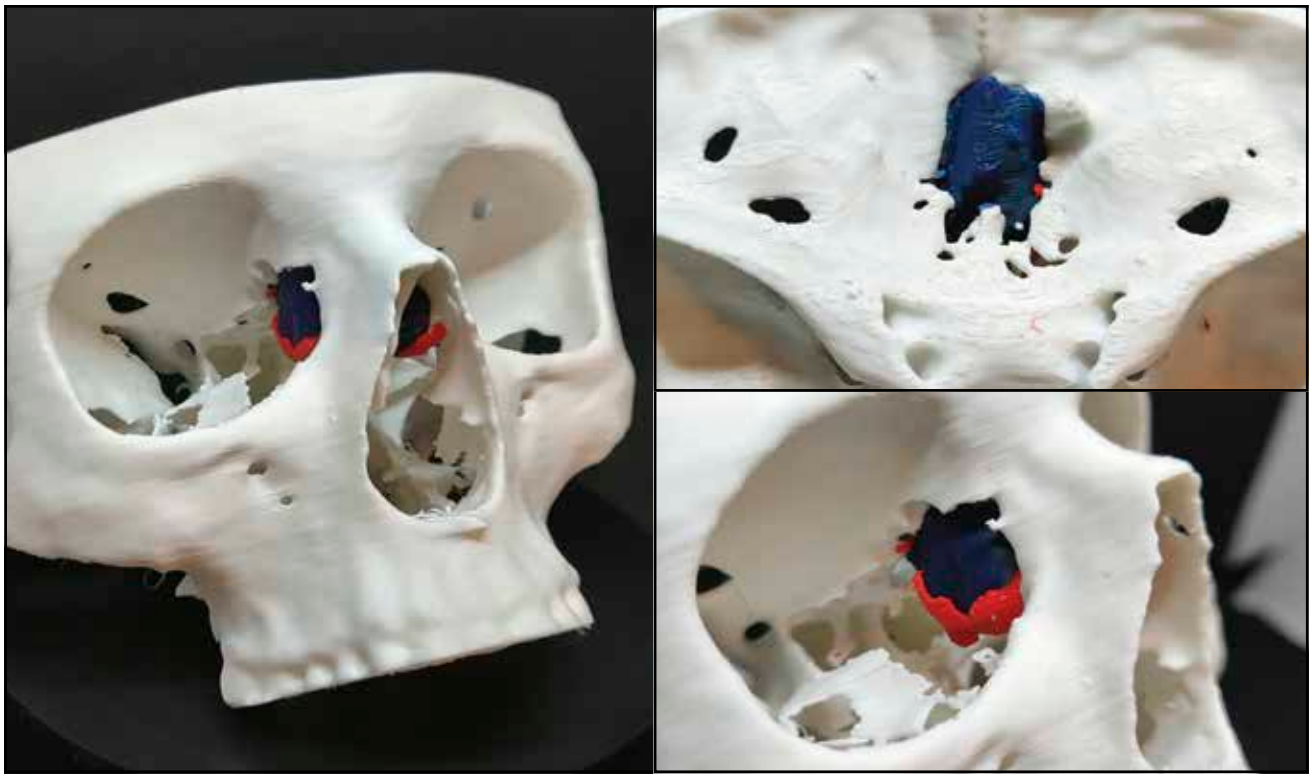

Figure 6. FDM-MMU 3D Printed model, showcasing the osteoma (blue) and 1-year follow-up extension (red), showing only the inferior extension, inside the nasal cavity.

scans to match and align to the other. After alignment, the two CT scans perfectly superimposed, and 3D automatic segmentation was performed. Osteomas are osseous tumours, so simple threshold segmentation was sufficient to perfectly separate them from the surrounding soft tissue. Differentiation between normal sinus walls and tumoral elements proved impossible to determine, as both types of tissue presented identical radiological absorption levels, and were visually indistinguishable on the CT scans. Initial 2D evaluation showed only a 2 mm average increase in the size of the tumour, with inferior extension inside the nasal cavity and no extension towards the endocranium (Figure 4). Next, 3D segmentations were reconstructed from the CT scans, to better showcase the tumour evolution from multiple angles. The resulting models were then digitally processed, with part of the orbit removed to better individualise the pathological process (Figure 5).

For the 3D printing of the models, given that the purpose of the model was as visual aid in presurgical planning (Figure 6), the same FDM-MMU and MSLA technologies discussed in Case 1 were chosen.

DISCUSSIONS

As previously discussed, challenges still persist in 3D segmentation and 3D printing of personalised models, in sinonasal pathologies. The small dimensions inherent to sinus bone structures result in low radio-absorption during CT scans and poor image differentiation on the resulting images. Automatic threshold 3D segmentation, while still providing a good amount of preliminary information, cannot reliably capture these small structures. Manual post-processing is still paramount, especially when segmenting structures around a tumour, with supplemental attention needed to separate tumoral limits from the surrounding structures.

Automated segmentation techniques, although advancing, still struggle with accurate delineation of complex anatomical structures, leading to potential inaccuracies in preoperative planning. Soft tissue tumours situated in the nasal cavity and paranasal sinuses can be difficult to differentiate from surrounding healthy structures, as they present similar densities. While MRI investigations can better separate tissues of similar density, an ability which a CT scan does not have, the big slice thickness and spacing result in a low resolution for segmentation, which is detrimental when attempting to segment the fine structures of the skull base. Even with good quality and large amounts of imaging data, manual segmentation is still required in a majority of sinonasal cases. This process is time-consuming and prone to user-dependent variability, which can affect the consistency and reliability of the 3D models.

Integrating data from different imaging modalities (e.g., CT, MRI), or from different acquisition times or devices remains a technical challenge. Each modality has its strengths and limitations, and combining these datasets into a coherent 3D model requires a sophisticated algorithm, especially if the alignment and integration is attempted on with different sources (CT scan and MRI combination, for example). Variability in CT imaging protocols and thresholding values can introduce significant cumulative spatial inaccuracies in the segmentation and 3D modelling process[15].

Despite promising advancements, many automated segmentation tools still require extensive clinical validation to ensure their reliability and accuracy in real-world surgical planning scenarios[16,17].

On the manufacturing side, 3D printing of these structures highlights 3D printing technology's ability to adapt to manufacture any shape. Especially in fine structures, such as those seen in paranasal sinuses' bones, MSLA 3D printing provides superior detail, but its inability to provide colours in the final models is a detriment in visual aid, both for medical professionals and for patient education.

CONCLUSIONS

Presurgical planning in sinonasal tumoral pathologies is a difficult endeavour that can greatly benefit from the integration of 3D segmentation and 3D printing technology. Through these two case reports presented in this article, it is evident that 3D printed models offer very good precision and clarity in visualizing complex anatomical structures, thus enhancing the accuracy of surgical planning and execution. The use of these models not only aids surgeons in meticulous preoperative assessment, but also serves as a valuable tool for patient follow-up and evaluation.

However, the practical implementation of 3D printing in sinonasal pathology faces several challenges. The intrinsic complexity of sinonasal anatomy requires high-resolution imaging and meticulous segmentation processes, often necessitating manual intervention to ensure accuracy, especially when differentiating between pathological and healthy during 3D segmentation. The integration of multiple imaging modalities and advancements in automated segmentation tools are crucial for overcoming these hurdles.

Despite these challenges, the benefits of 3D printing in sinonasal surgery are evident. The technology allows the creation of real 1:1 replicas of the anatomy and pathology of the patient, offering much more information than a 2D CT or MRI scan can offer. Moreover, the replicability of 3D printed models in medical training provides a realistic and safe environment for training surgeons to hone their skills on complex, often one-of-a-kind cases.

Future directions in this field should focus on refining imaging and segmentation techniques, improving the accuracy and reliability of automated tools, especially at differentiating fine bone lamella from surrounding soft tissue. With continued advancements and clinical validation, 3D printing is already a mainstay in presurgical planning and patient education, leading to better patient outcomes and more efficient healthcare delivery.

Funding: Research carried out in the 3D Printing Lab, part of the Center of Innovation and e-Health of the "Carol Davila" University of Medicine and Pharmacy in Bucharest, within the research project "InnovaMed-Praxis: integrated platform for advanced medical practice" funded by the Ministry of Education from the Institutional Development Fund for state universities; project code CNFIS-FDI-2024-0592.

Contribution of authors: All authors equally contributed.

Conflicts of interest: The authors declared no potential conflicts of interest with respect to the research, authorship, and/or publication of this article.

Acknowledgments: All materials and 3D manufacturing devices mentioned in the article belong to the 3D Printing Lab at the Center of Innovation and e-Health part of "Carol Davila" University of Medicine and Pharmacy, Bucharest, Romania.

Financial disclosure: None.

Authors' information

Dragomir Mihai, PhD student, ENT Resident, ENT&HNS Department, CESITO Center, "Sfanta Maria" Hospital, Bucharest, Romania; 3D Printing Lab, Center of Innovation and e-Health, "Carol Davila" University of Medicine and Pharmacy, Bucharest, Romania. E-mail: mihai.dragomir@umfcd.ro. ORCID: https://orcid.org/0009-0007-3841-6748.

Codrut Sarafoleanu, Professor of Otorhinolaryngology, ENT&HNS Department, CESITO Center, "Sfanta Maria" Hospital, "Carol Davila" University of medicine and Pharmacy, Bucharest, Romania. E-mail: csarafoleanu@gmail.com. ORCID: https://orcid.org/0000-0002-9436-7772.

Liciu Eduard, PhD in Medicine, Orthopedic surgeon, Coordinator of the 3D Printing Lab at the Center of Innovation and e-Health, "Carol Davila" University of Medicine and Pharmacy, Bucharest, Romania. E-mail: eduard.liciu@drd.umfcd.ro. ORCID: https://orcid.org/0000-0003-2323-6959.

Cristea Daniel, Engineer, PhD student, Master's degree in medical engineering, 3D Printing Lab, Center of Innovation and e-Health, "Carol Davila" University of Medicine and Pharmacy, Bucharest, Romania. E-mail: doru.cristea@umfcd.ro. ORCID: https://orcid.org/0009-0007-9906-1290.

REFERENCES

1. Fitzgerald CW, Hararah M, Mclean T, Woods R, Dogan S, Tabar V, et al. Virtual surgical planning and three-dimensional models for precision sinonasal and skull base surgery. Cancers (Basel). 2023;15(20):4989. DOI: 10.3390/cancers15204989.
2. Sander IM, Liepert TT, Doney EL, Leevy WM, Liepert DR. Patient education for endoscopic sinus surgery: Preliminary experience using 3D-printed clinical imaging data. J Funct Biomater. 2017;8(2):13. DOI: 10.3390/jfb8020013.
3. Tevanov I, Liciu E, Chirila MO, Dusca A, Ulici A. The use of 3D printing in improving patient-doctor relationship and malpractice prevention. Romanian J Leg Med. 2017;25(3):279-82. DOI: 10.4323/rjlm.2017.279.
4. Rose AS, Webster CE, Harrysson OLA, Formeister EJ, Rawal RB, Iseli CE. Pre-operative simulation of pediatric mastoid surgery with 3D-printed temporal bone models. Int J Pediatr Otorhinolaryngol. 2015;79(5):740-4. DOI: 10.1016/j.ijporl.2015.03.004.
5. Zhuo C, Lei L, Yulin L, Wentao L, Shuangxia W, Chao W, et al. Creation and validation of three-dimensional printed models for basic nasal endoscopic training. Int Forum Allergy Rhinol. 2019;9(6):695-701. DOI: 10.1002/alr.22306.
6. Liciu E, Frumuseanu B, Popescu BM, Florea DC, Niculescu L, Ulici A. Personalized surgical planning – the use of 3D printing in oncological pathology. Romanian J Orthop Surg Traumatol. 2018;1(Supplement):40-40. DOI: 10.2478/rojost-2018-0051.
7. Jing Z, Zhang T, Xiu P, Cai H, Wei Q, Fan D, et al. Functionalization of 3D-printed titanium alloy orthopedic implants: a literature review. Biomed Mater. 2020;15(5):052003. DOI: 10.1088/1748-605X/ab9078.
8. Simal I, Garcia-Casillas MA, Cerda JA, Riquelme O, Lorca-Garcia C, Perez-Egido L, Fernandez-Bautista B, et al. Three-dimensional custom-made titanium ribs for reconstruction of a large chest wall defect. European J Pediatr Surg Rep. 2016;4(1):26-30. DOI: 10.1055/s-0036-1593738.
9. Zhai Y, Zhang H, Wang J, Zhao D. Research progress of metal-based additive manufacturing in medical implants. Reviews on Advanced Materials Science. 2023;62(1):20230148. DOI: 10.1515/rams-2023-0148.
10. Ng SL, Das S, Ting YP, Wong RCW, Chanchareonsook N. Benefits and biosafety of use of 3D-printing technology for titanium biomedical implants: A pilot study in the rabbit model. Int J Mol Sci. 2021;22(16):8480. DOI: 10.3390/ijms22168480.
11. 3D Slicer image computing platform. [Internet]. Available from: https://www.slicer.org/.
12. Blender. [Internet]. Version 3.1.0. Released March 9th, 2022. Available from: https://www.blender.org/download/releases/3-1/.
13. Bambu Studio. [Internet]. Bambu Lab. Available from: https://bambulab.com/en-eu/download/studio.
14. Anycubic MonoX2. Aycubic [3D Printer]. Available from: https://store.anycubic.com/products/photon-mono-x2-sla-3d-printer.
15. Akmal JS, Salmi M, Hemming B, Teir L, Soumalainen A, Kortesniemi M, et al. Cumulative inaccuracies in implementation of additive manufacturing through medical imaging, 3D thresholding, and 3D modeling: A case study for an end-use implant. Appl Sci Switz. 2020;10(8):2968. DOI: 10.3390/app10082968.
16. Deng Z, Wang B, Zhu Z. BE-FNet: 3D bounding box estimation feature pyramid network for accurate and efficient maxillary sinus segmentation. Math Probl Eng. 2020;2020:1-6. DOI: 10.1155/2020/5689301.
17. Yang G, Dai Z, Zhang Y, Zhu L, Tan J, Chen Z, et al. Multiscale local enhancement deep convolutional networks for the automated 3D segmentation of gross tumor volumes in nasopharyngeal carcinoma: a multi-institutional dataset study. Front Oncol. 2022;12:827991. DOI: 10.3389/fonc.2022.827991.